Proton Nonionizing Energy Loss (NIEL) for Device Applications

Insoo Jun, Michael A. Xapsos, Scott R. Messenger, Edward A. Burke, Robert J. Walters, Geoff P. Summers, and Thomas Jordan

Abstract--**The proton induced NIEL for representative device materials are presented for the energy range between 1 keV to 1000 MeV. All interaction mechanisms (Coulomb and nuclear elastic/inelastic) are fully accounted for in the present NIEL calculations. For Coulomb interactions, the Ziegler, Biersack, Littmark (ZBL) screened potential was used in the lower energy range (< 50MeV) and the relativistic formulation was used in the higher energy range (≥ 50MeV). A charged particle transport code, MCNPX, was used to compute the NIEL due to nuclear interactions.**

I. INTRODUCTION

NONIONIZING energy loss (NIEL) is a quantity that describes the rate of energy loss due to atomic displacements as a particle traverses a material. The product of the NIEL and the particle fluence (time integrated flux) gives the displacement damage energy deposition per unit mass of material. NIEL plays the same role to the displacement damage energy deposition as the stopping power to the total ionizing dose (TID). The concept of NIEL has been very useful for correlating particle induced displacement damage effects in semiconductor and optical devices. Many studies have successfully demonstrated that the degradation of semiconductor devices or optical sensors in a radiation field can be linearly correlated to the displacement damage energy, and subsequently to the NIEL deposited in the semiconductor devices or optical sensors [1]-[3]. In addition, the NIEL concept was also useful in the study of both Si and GaAs solar cells [4]-[7] and of high temperature superconductors [8], and at predicting the survivability of detectors used at the LHC at CERN. On the other hand, there are some instances where discrepancies are observed in the application of NIEL, most notably in GaAs semiconductor devices [9]. However, NIEL is still a valuable tool, and can be used to scale damages produced by different particles and in different environments, even though this is not understood at the microscopic level [10].

Despite the general acceptance of the NIEL approach there are problems that hinder its widespread use. First, the number of cases where extensive calculations and data are available remains limited. Of particular concern to the radiation effects community is the lack of information for current device materials. Further, the number and diversity of material and device types continues to increase. NIEL can be particularly helpful for analyzing damage in new devices where limited radiation data are available. This is part of an ongoing effort to solve this situation under the NASA Space Environments and Effects program and the NASA Living With a Star Space Environment Testbed program. Particularly, this paper presents calculated results for proton NIEL in 10 materials relevant for current and emerging device technologies - C, Al, Si, P, Ga, Ge, As, In, Cu and Se. These results can also easily be used to obtain NIEL for compound materials composed of any number of the 10 elements. Proton energies covered in this study are from 1 keV to 1000 MeV.

When protons traverse a material, they interact through atomic Coulombic interactions, and nuclear elastic/inelastic reactions. At energies below about 10 MeV, Coulombic interactions dominate the production of displaced atoms from their lattice sites. At energies above 30-50 MeV, nuclear reactions are mostly responsible for displacements. Evaluation of the proton NIEL should involve proper treatment of each type of interaction. A feature of this work is the use of the charged particle Monte Carlo transport code, MCNPX [12], for the nuclear interactions, which allows tracking of primary and secondary particles (up to helium ions) from the proton interactions. Descriptions of the relevant physics and methods are described in Section II and III, followed by results in Section IV.

Manuscript received July 22, 2003. The authors would like to acknowledge both the NASA SEE and SET programs for the funding of this work. A part of the research described in this paper was carried out at the Jet Propulsion Laboratory, California Institute of Technology, under a contract with the National Aeronautics and Space Administration.

Insoo Jun is with the Jet Propulsion Laboratory, California Institute Of Technology, Pasadena, CA 91109-8099, USA (telephone: 818-354-7107, e-mail: Insoo.Jun@jpl.nasa.gov).

Michael A. Xapsos is with GFSC/NASA, Greenbelt, MD 20771, USA (telephone: 301-286-2263, e-mail: Michael.A.Xapsos@nasa.gov).

Scott R. Messenger is with SFA, Inc., Largo, MD 20774, USA (telephone: 202-767-7360, e-mail: messenger@nrl.navy.mil).

Edward A. Burke is a Consultant, Woburn, MA 01801, USA (telephone: 781-933-2900, e-mail: edaburke@rcn.com).

Robert J. Walters is with US Naval Research Laboratory, Washington, DC 20375, USA (telephone: 202-767-2533, e-mail: rwalters@ccf.nrl.navy.mil).

Geoff P. Summers is with US Naval Research Laboratory, Washington, DC 20375, USA (telephone: 202-7672446, e-mail: gsummers@ccf.nrl.navy.mil).

Thomas Jordan is with EMP Consultants, Gaithersburg, MD 20885, USA (telephone: 301-869-2317, e-mail: tj@empc.com).

II. ATOMIC COULOMB INTERACTIONS

The classical Rutherford scattering formula has been widely used for computing the Coulomb contribution to proton NIEL. However, the straightforward application of the classical formulation over the entire energy range covered in this study (1 keV to 1000 MeV) is not appropriate for the proper evaluation of NIEL, especially in the low energy region where a screened potential (a reduction of the Coulomb potential because of the electrostatic screening of the nuclear charges by the space charge of the innermost electron shells) should be used [11]. In addition, in the high energy region a relativistic treatment of the scattering process is more appropriate. In this study, we successfully used the Ziegler, Biersack, Littmark (ZBL) screened Coulomb potential [11], [13] coupled to the relativistic energy transfer cross section at higher incident energies [14]. Typical results between 1 keV to 1000 MeV are shown in Fig. 1 for silicon. The corrections to the classical Coulomb scattering cross section are evident at the lowest and highest energies shown.

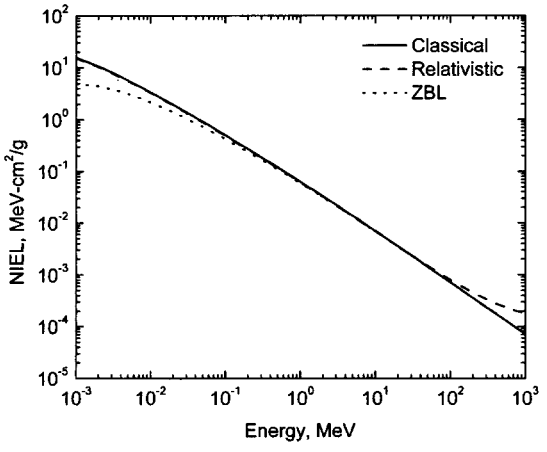

Fig. 1. Proton NIEL for silicon due the Coulomb scattering, computed using three different formalisms.

III. NUCLEAR INTERACTIONS

Recently, Jun [14] described a method to compute the nuclear contribution to proton NIEL by using a charged particle transport code, MCNPX, based on the thin target approximation. A thin (relative to the CSDA range of incident protons) slab of material of interest with a normalized density of 0.01 atoms/barn-cm was modeled, and a pencil beam of protons was simulated penetrating the slab. Using the damage energy tally, then the history tape written by MCNPX was analyzed to calculate the mean damage energy per source particle, T_{dam}, which is the nonionizing portion of the energy deposited (i.e., after Lindhard partition function applied). The damage energy cross section, σ_d, is given by: $\sigma_d = T_{dam}/(N_v x)$ where N_v is the atom density and x is the target thickness. Then, NIEL is related to the damage energy cross section: $S_{NIEL} = (N/A)\sigma_d$ where N is the Avogadro's number and A is the gram atomic weight of the target material. By using MCNPX, we were able to compute the nuclear contributions

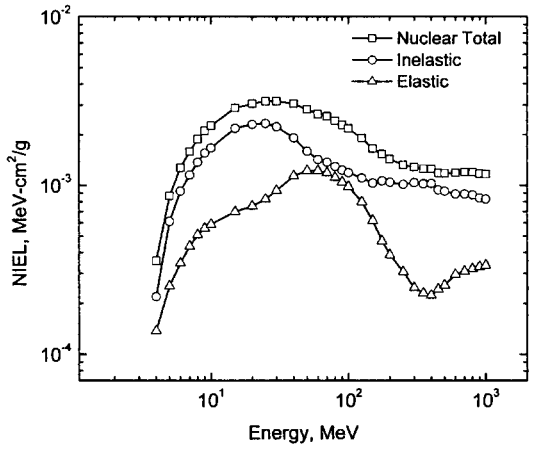

Fig. 2. Proton NIEL for silicon due to the nuclear interactions.

to the proton NIEL for many materials. Fig. 2 illustrates the results for silicon, which shows the separate contributions of nuclear elastic and inelastic interactions. When a proton comes in the problem geometry and makes a collision, MCNPX uses the cross sections by Barashenkov and Polanski [15] to determine elastic and non-elastic reaction probabilities. If elastic, MCNPX computes the primary knock-on (PKA) energy using standard kinematics. If non-elastic reaction, MCNPX goes to the high energy intra-nuclear cascade (INC)/pre-equilibrium/evaporation physics to compute the PKA energy. The physics of these processes are well documented in [12] and references therein. The following discussion is mainly from [12] and included here to provide readers brief descriptions of the processes relevant to our study.

In the INC stage, the high energy incident particle undergoes a series of direct reactions inside the target nucleus. High-energy secondary particles (or small group of nucleons and mesons) and low-energy cascade particles are ejected from the nucleus leaving the nucleus in a highly excited state. We used the Bertini INC model [16,17] implemented in MCNPX. Subsequent de-excitation of the residual nucleus after the INC phase employs a multi-stage, multi-step pre-equilibrium exciton model, or MPM [18]. The MPM is invoked at the completion of the INC, with an initial particle-hole configuration and excitation energy determined by the outcome of the cascade. At each stage in the MPM, the excited nucleus may emit a neutron, proton, deuteron, triton, helium-3 or alpha; alternatively, the nuclear configuration may evolve toward and equilibrium exciton number by increasing the exciton number by one particle-hole pair. The MPM terminates upon reaching the equilibrium exciton number, at which an evaporation model is then applied to the residual nucleus with the remaining excitation energy. MCNPX uses the Dresner evaporation model [19], based on work originally due to Weisskopf [20]. After the INC/MPM stage, residual nuclei are in highly excited states, and energy is dissipated by evaporation of neutrons, protons, deuterons,

tritons, helium-3's and alphas. Note that the Fermi breakup model [21] replaces the evaporation model for the disintegration of light nuclei in MCNPX. It treats the de-excitation process as a sequence of simultaneous breakups of the excited nucleus into two or more products, each of which may be a stable or unstable nucleus or nucleon. Any unstable product nucleus is subject to subsequent breakup. The model is applied only for residual nuclei with A≤17, replacing the evaporation model for these nuclei.

IV. RESULTS

We first compare our new results to a previous study. Fig. 3 shows proton NIEL for Si compared to the values in [6]. The results of the calculations are in very good agreement except at the very lowest proton energies, where our use of a screened Coulomb potential results in lower NIEL values. Similar results are seen for GaAs and InP, except that this effect is more pronounced due to the higher Z values of the materials, as shown in Fig. 4 for the GaAs NIEL. The very good agreement at high proton energies verifies previous results and gives us confidence that the MCNPX code is a useful tool for this purpose.

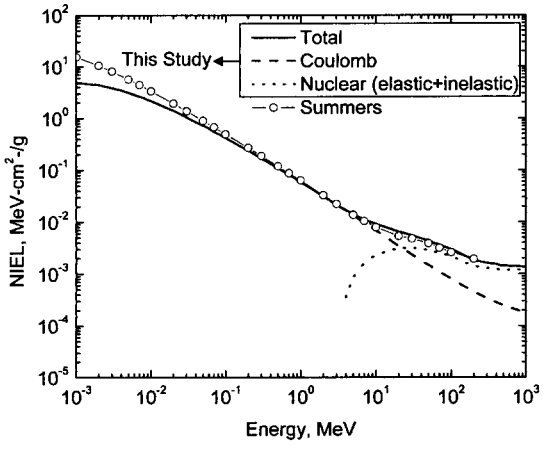

Fig. 3. Proton NIEL for Si obtained in this study, compared to the Summers et al. results [6]. For the Coulomb contribution, the ZBL screened Coulomb potential was used for E<50 MeV, and relativistic energy transfer cross section was used for E≥50 MeV.

Figs. 5 and 6 show results for the proton NIELs in all 10 materials selected for this study: carbon, aluminum, silicon, phosphorous, gallium, copper, germanium, arsenic, selenium, and indium. The numerical data are also presented in Table I at selected energies. These materials were chosen specifically because they are used in the fabrication of devices. It is also straight-forward to obtain NIEL for a compound composed of 2 or more of these materials by weighting the NIEL value given for each material by the gram atomic weight. This procedure has also been verified by a direct computation of NIEL for compounds. Thus, the 10 material results should provide researchers with considerable flexibility.

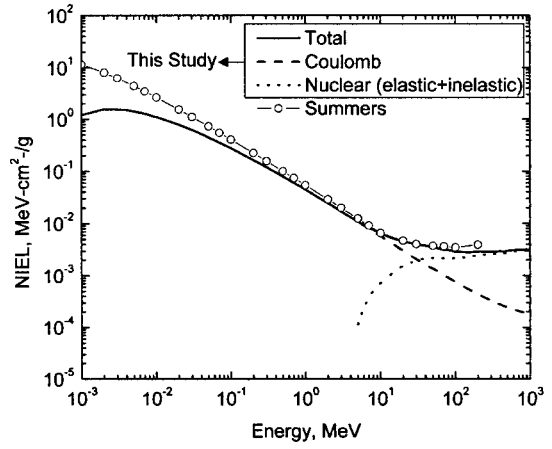

Fig. 4. Proton NIEL for GaAs obtained in this study, compared to the Summers et al. results [6]. See the Fig. 3 caption for the description of Coulomb NIEL calculations.

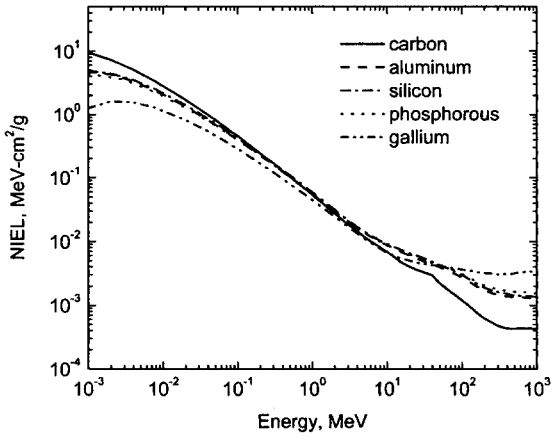

Fig. 5. Proton NIELs obtained in this study for C, Al, Si, P and Ga. The results shown include the contributions of Coulomb and nuclear interactions. See the Fig. 3 caption for the description of Coulomb NIEL calculations.

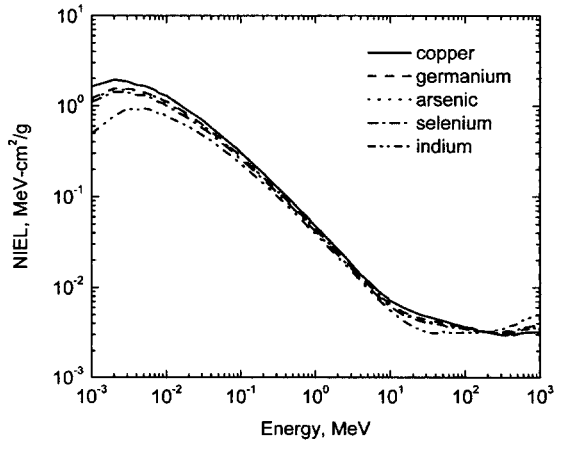

Fig. 6. Proton NIELs obtained in this study for Cu, Ge, As, Se, and In. The results shown include the contributions of Coulomb and nuclear interactions. See the Fig. 3 caption for the description of Coulomb NIEL calculations.

TABLE I

NUMERICAL NONIONIZING ENERGY LOSS (NIEL) IN MEV-CM^2/G FOR THE 10 MATERIALS STUDIED IN THIS PAPER. THE VALUES SHOWN INCLUDE THE CONTRIBUTIONS FROM COULOMBIC INTERACTIONS AS WELL AS NUCLEAR ELASTIC AND INELASTIC INTERACTIONS.

Energy, MeV	Carbon	Aluminum	Silicon	Phosphorous	Gallium	Germanium	Arsenic	Indium	Copper	Selenium
0.001	9.52	4.75	4.88	4.39	1.26	1.21	1.18	4.94×10^{-1}	1.64	1.10
0.002	7.30	4.28	4.44	3.83	1.61	1.56	1.53	7.73×10^{-1}	1.94	1.43
0.003	5.89	3.70	3.86	3.53	1.58	1.54	1.50	9.34×10^{-1}	1.86	1.41
0.005	4.41	2.98	3.13	2.77	1.45	1.42	1.39	9.39×10^{-1}	1.67	1.31
0.007	3.57	2.52	2.65	2.36	1.32	1.29	1.27	8.45×10^{-1}	1.50	1.14
0.01	2.80	2.06	2.17	1.95	1.14	1.12	1.10	7.70×10^{-1}	1.29	1.00
0.02	1.70	1.33	1.41	1.27	8.14×10^{-1}	8.00×10^{-1}	7.64×10^{-1}	5.90×10^{-1}	8.79×10^{-1}	7.26×10^{-1}
0.03	1.23	9.94×10^{-1}	1.06	9.60×10^{-1}	6.38×10^{-1}	6.27×10^{-1}	6.21×10^{-1}	4.77×10^{-1}	7.07×10^{-1}	5.73×10^{-1}
0.05	8.17×10^{-1}	6.86×10^{-1}	7.32×10^{-1}	6.67×10^{-1}	4.62×10^{-1}	4.55×10^{-1}	4.39×10^{-1}	3.58×10^{-1}	4.95×10^{-1}	4.18×10^{-1}
0.07	6.19×10^{-1}	5.31×10^{-1}	5.54×10^{-1}	5.19×10^{-1}	3.68×10^{-1}	3.53×10^{-1}	3.51×10^{-1}	2.91×10^{-1}	3.94×10^{-1}	3.35×10^{-1}
0.1	4.56×10^{-1}	4.01×10^{-1}	4.19×10^{-1}	3.93×10^{-1}	2.85×10^{-1}	2.75×10^{-1}	2.73×10^{-1}	2.30×10^{-1}	3.05×10^{-1}	2.61×10^{-1}
0.2	2.41×10^{-1}	2.23×10^{-1}	2.39×10^{-1}	2.25×10^{-1}	1.66×10^{-1}	1.64×10^{-1}	1.63×10^{-1}	1.41×10^{-1}	1.81×10^{-1}	1.56×10^{-1}
0.3	1.70×10^{-1}	1.61×10^{-1}	1.69×10^{-1}	1.60×10^{-1}	1.22×10^{-1}	1.18×10^{-1}	1.18×10^{-1}	1.03×10^{-1}	1.30×10^{-1}	1.13×10^{-1}
0.5	1.03×10^{-1}	1.01×10^{-1}	1.09×10^{-1}	1.03×10^{-1}	7.93×10^{-2}	7.86×10^{-2}	7.83×10^{-2}	6.93×10^{-2}	8.61×10^{-2}	7.50×10^{-2}
0.7	7.55×10^{-2}	7.55×10^{-2}	8.15×10^{-2}	7.72×10^{-2}	6.02×10^{-2}	5.96×10^{-2}	5.94×10^{-2}	5.30×10^{-2}	6.52×10^{-2}	5.70×10^{-2}
1	5.37×10^{-2}	5.48×10^{-2}	5.93×10^{-2}	5.63×10^{-2}	4.45×10^{-2}	4.41×10^{-2}	4.40×10^{-2}	3.95×10^{-2}	4.81×10^{-2}	4.22×10^{-2}
2	2.76×10^{-2}	2.91×10^{-2}	3.16×10^{-2}	2.95×10^{-2}	2.45×10^{-2}	2.44×10^{-2}	2.43×10^{-2}	2.16×10^{-2}	2.65×10^{-2}	2.29×10^{-2}
3	1.85×10^{-2}	2.02×10^{-2}	2.15×10^{-2}	2.08×10^{-2}	1.71×10^{-2}	1.70×10^{-2}	1.69×10^{-2}	1.55×10^{-2}	1.84×10^{-2}	1.63×10^{-2}
5	1.17×10^{-2}	1.37×10^{-2}	1.42×10^{-2}	1.36×10^{-2}	1.10×10^{-2}	1.09×10^{-2}	1.09×10^{-2}	9.75×10^{-3}	1.19×10^{-2}	1.03×10^{-2}
7	8.99×10^{-3}	1.08×10^{-2}	1.13×10^{-2}	1.08×10^{-2}	8.47×10^{-3}	8.40×10^{-3}	8.34×10^{-3}	7.33×10^{-3}	9.04×10^{-3}	7.86×10^{-3}
10	6.86×10^{-3}	8.73×10^{-3}	9.14×10^{-3}	8.73×10^{-3}	6.66×10^{-3}	6.57×10^{-3}	6.51×10^{-3}	5.55×10^{-3}	7.15×10^{-3}	6.13×10^{-3}
20	3.98×10^{-3}	6.00×10^{-3}	6.49×10^{-3}	6.19×10^{-3}	4.99×10^{-3}	4.83×10^{-3}	4.71×10^{-3}	3.70×10^{-3}	5.41×10^{-3}	4.55×10^{-3}
30	3.31×10^{-3}	4.95×10^{-3}	5.51×10^{-3}	5.16×10^{-3}	4.46×10^{-3}	4.41×10^{-3}	4.23×10^{-3}	3.21×10^{-3}	4.81×10^{-3}	4.09×10^{-3}
50	2.20×10^{-3}	3.96×10^{-3}	4.30×10^{-3}	4.36×10^{-3}	4.19×10^{-3}	4.16×10^{-3}	4.04×10^{-3}	3.24×10^{-3}	4.29×10^{-3}	3.86×10^{-3}
70	1.62×10^{-3}	3.32×10^{-3}	3.65×10^{-3}	3.72×10^{-3}	3.90×10^{-3}	3.84×10^{-3}	3.73×10^{-3}	3.14×10^{-3}	3.92×10^{-3}	3.62×10^{-3}
100	1.18×10^{-3}	2.70×10^{-3}	2.97×10^{-3}	3.08×10^{-3}	3.62×10^{-3}	3.60×10^{-3}	3.58×10^{-3}	3.18×10^{-3}	3.64×10^{-3}	3.46×10^{-3}
200	6.20×10^{-4}	1.72×10^{-3}	1.88×10^{-3}	2.03×10^{-3}	3.20×10^{-3}	3.24×10^{-3}	3.28×10^{-3}	3.25×10^{-3}	3.17×10^{-3}	3.21×10^{-3}
300	4.74×10^{-4}	1.47×10^{-3}	1.62×10^{-3}	1.79×10^{-3}	3.03×10^{-3}	3.13×10^{-3}	3.13×10^{-3}	3.39×10^{-3}	2.99×10^{-3}	3.14×10^{-3}
500	4.26×10^{-4}	1.34×10^{-3}	1.43×10^{-3}	1.63×10^{-3}	3.17×10^{-3}	3.27×10^{-3}	3.28×10^{-3}	4.02×10^{-3}	3.06×10^{-3}	3.42×10^{-3}
700	4.29×10^{-4}	1.32×10^{-3}	1.41×10^{-3}	1.61×10^{-3}	3.32×10^{-3}	3.47×10^{-3}	3.54×10^{-3}	4.54×10^{-3}	3.20×10^{-3}	3.67×10^{-3}
1000	4.21×10^{-4}	1.29×10^{-3}	1.34×10^{-3}	1.54×10^{-3}	3.34×10^{-3}	3.50×10^{-3}	3.58×10^{-3}	4.96×10^{-3}	3.14×10^{-3}	3.75×10^{-3}

IV. CONCLUSIONS

The computation of proton induced NIEL for 10 materials of interest to the space environment community have been carried out using state-of-the-art methods. Results for a number of these materials were not previously available. The proton energies covered are from 1 keV to 1000 MeV. The ZBL screened potential and the relativistic kinematics were used to compute the Coulomb contribution to NIEL. For the nuclear elastic and inelastic interactions, a MCNPX method (thin target approximation) was used. It was shown that in lower energy region, the use of the screened potential is very important to evaluate proper NIELs. At high energies, the results of this study agree very well with previous results, which validates our method to compute the high energy NIELs (relativistic Coulomb and MCNPX for nuclear interactions).

V. REFERENCES

[1] G. R. Hopkinson, C. J. Dale, and P. W. Marshall, "Proton Effects in Charged-Coupled Devices," *IEEE Trans. on Nucl. Sci.*, Vol. 43, No. 2, April 1996.

[2] J. Janesick, T. Elliott, and F. Pool, "Radiation Damage in Scientific Charge-Coupled Devices," *IEEE Trans. on Nucl. Sci.*, Vol. 36, No. 1, February 1989.

[3] C. Dale, P. Marshall, B. Cummings, L. Shamey, and A. Holland, "Displacement Damage Effects in Mixed Particle Environments for Shielded Spacecraft CCDs," *IEEE Trans. on Nucl. Sci.*, Vol. 40, No. 6, December 1993.

[4] G. P. Summers, R. J. Walters, M. A. Xapsos, E. A. Burke, S. R. Messenger, P. Shapiro, and R. L. Statler, "A New Approach to Damage Prediction for Solar Cells Exposed to Different Radiations," *Proc. 1st IEEE World Conference on Photovoltaic Energy Conversion*, Waikoloa, Hawaii, pp. 2068-2075, December 1994.

[5] S. R. Messenger, G. P. Summers, E. A. Burke, R. J. Walters, and M. A. Xapsos, "Modeling Solar Cell Degradation in Space: A Comparison of the NRL Displacement Damage Dose and the JPL Equivalent Fluence Approaches," *Progress Photovoltaics*, Vol. 9, pp. 103-121, 2001.

[6] G. P. Summers, E. A. Burke, P. Shapiro, S. R. Messenger, and R. J. Walters, "Damage Correlations in Semiconductors Exposed to Gamma,

Electron, and Proton Radiations," *IEEE Trans. on Nucl. Sci.*, Vol. 40, pp. 1372-1379, December 1993.

[7] S. R. Messenger, M. A. Xapsos, E. A. Burke, R. J. Walters, and G. P Summers, "Proton Displacement Dmage and Ionizing Dose for Shielded Devices in Space," *IEEE Trans. on Nucl. Sci.*, Vol. 47, pp. 2169-2173, December 1997.

[8] B. D. Weaver, E. M. Jackson, G. P. Summers, and E. A. Burke, "Atomic Disorder and the Transition Temperature of Cuprate Superconductors," Phys. Rev., Vol. B46, pp. 1134-1137, 1992.

[9] S. R. Messenger, R. J. Walters, E. A. Burke, G. P. Summers, and M. A. Xapsos, "NIEL and Damage Correlations for High-Energy Protons in Gallium Arsenide Devices," *IEEE Trans. on Nucl. Sci.*, Vol. 48, pp. 2121-2126, December 2001.

[10] M. Huhtinen, "Simulation of Nonionizing Energy Loss and Defect Formation in Silicon," *Nuclear Instruments and Methods in Physics Research*, Vol. A491, pp. 194-215, 2002.

[11] J. F. Ziegler, J. P. Biersack, and U. Littmark, *The Stopping and Range of Ions in Solids*, Volume 1 of The Stopping and Ranges of ions in Matter, edited by J.F. Ziegler, Pergamon Press, 1985.

[12] "MCNPX User's Manual: Version 2.4.0," LA-CP-02-408, Los Alamos National Lab., September 2002.

[13] S. R. Messenger, E. A. Burke, M. A. Xapsos, G. P. Summers, R. J. Walters, I. Jun and T. Jordan, "NIEL for Heavy Ions: An Analytical Approach", submitted to this conference.

[14] I. Jun, "Effects of Secondary Particles on the Total Dose and the Displacement Damage in Space Proton Environment," *IEEE Trans. on Nucl. Sci.*, Vol. 48, pp. 162-175, February 2001.

[15] V. S. Barashenkov and A. Polanski, "Electronic Guide for Nuclar Cross-Sections," Comm. JINR E2-94-417, Dubna, 1994.

[16] H. W. Bertini, "Low-Energy Intranuclear Cascade Calculation," Physical Review, Vol. 131, No. 4, pp. 1801-1821, 1963.

[17] H. W. Bertini, "Intranuclear-Cascade Calculation of the Secondary Nucleon Spectra from Nucleon-Nucleus Interactions in the Energy Rage 340 to 2900 MeV and Comparisons with Experiments," Physical Review, Vol. 188, No. 4, pp. 1711-1730, 1969.

[18] R. E. Prael and M. Bozoian, "Adaptation of the Multistage Pre-equilibrium Model for the Monte Carlo Method (I)," Los Alamos National Laboratory Report, LA-UR-88-3238, 1998.

[19] L. Dresner, "EVAP – A Fortran Program for Calculating the Evaporation of Various Particles from Excited Compound Nuclei," Oak Ridge National Laboratory Report, ORNL-TM-7882, 1981.

[20] V. Weisskopf, "Statistics and Nuclear Reactions," Physical Review, Vol. 52, pp. 295-303, 1937.

[21] D. J. Brenner, R. E. Prael, J. F. Dicello, and M. Zaider, "Improved Calculations of Energy Deposition from Fast Neutrons," Proceedings of Fourth Symposium on Neutron Dosimetry, EUR-7448, Munich-Neuherberg, 1981.